

Title: Low Energy Spin Excitations in Chromium Metal

CONF-970452--

Author(s): Roger Pynn
R.T. Azuah
W.G. Stirling
Jiri Kulda

RECEIVED
OCT 08 1998
OSTI

Submitted to: NATO Advanced Study Institute on
Dynamical Properties of Unconventional
Magnetic Systems

DISTRIBUTION OF THIS DOCUMENT IS UNLIMITED *ph*

MASTER

Los Alamos

NATIONAL LABORATORY

Los Alamos National Laboratory, an affirmative action/equal opportunity employer, is operated by the University of California for the U.S. Department of Energy under contract W-7405-ENG-36. By acceptance of this article, the publisher recognizes that the U.S. Government retains a nonexclusive, royalty-free license to publish or reproduce the published form of this contribution, or to allow others to do so, for U.S. Government purposes. Los Alamos National Laboratory requests that the publisher identify this article as work performed under the auspices of the U.S. Department of Energy. The Los Alamos National Laboratory strongly supports academic freedom and a researcher's right to publish; as an institution, however, the Laboratory does not endorse the viewpoint of a publication or guarantee its technical correctness.

DISCLAIMER

This report was prepared as an account of work sponsored by an agency of the United States Government. Neither the United States Government nor any agency thereof, nor any of their employees, makes any warranty, express or implied, or assumes any legal liability or responsibility for the accuracy, completeness, or usefulness of any information, apparatus, product, or process disclosed, or represents that its use would not infringe privately owned rights. Reference herein to any specific commercial product, process, or service by trade name, trademark, manufacturer, or otherwise does not necessarily constitute or imply its endorsement, recommendation, or favoring by the United States Government or any agency thereof. The views and opinions of authors expressed herein do not necessarily state or reflect those of the United States Government or any agency thereof.

DISCLAIMER

Portions of this document may be illegible in electronic image products. Images are produced from the best available original document.

LOW ENERGY SPIN EXCITATIONS IN CHROMIUM METAL

ROGER PYNN¹, R. T. AZUAH², W. G. STIRLING³, and JIRI KULDA⁴

¹*Los Alamos National Laboratory, Los Alamos, New Mexico 87544, U.S.A.*

²*Hahn-Meitner-Institut, Glienicker Strasse 100, 14109 Berlin, Germany*

³*Department of Physics, University of Liverpool, Oxford St., Liverpool L69 3BX, U.K.*

⁴*Institut Laue Langevin, Grenoble, France*

1. Abstract

Neutron scattering experiments with full polarization analysis have been performed with a single crystal of chromium to study the low-energy spin fluctuations in the transverse spin density wave (TSDW) state. A number of remarkable results have been found. Inelastic scattering observed close to the TSDW satellite positions at $(1 \pm \delta, 0, 0)$ does not behave as expected for magnon scattering. In particular, the scattering corresponds to almost equally strong magnetization fluctuations both *parallel* and *perpendicular* to the ordered moments of the TSDW phase. As the Neel temperature is approached from below, scattering at the commensurate wavevector $(1, 0, 0)$ increases in intensity as a result of critical scattering at "silent" satellites $(1, 0, \pm \delta)$ being included within the spectrometer resolution function. This effect, first observed by Sternlieb et al, does not account for all of the inelastic scattering around the $(1, 0, 0)$ position, however. Rather, there are further collective excitations, apparently emanating from the TSDW satellites, which correspond to magnetic fluctuations *parallel* to the ordered TSDW moments. These branches have a group velocity that is close to that of $(1, 0, 0)$ longitudinal acoustic (LA) phonons, but assigning their origin to magneto-elastic scattering raises other unanswered questions.

2. The Static Magnetic Structure of Chromium Metal

Metallic chromium is a remarkable metal [1]. Below its Neel temperature, T_N , of 311 K, it has a magnetic structure which is *almost* antiferromagnetic, but not quite. Instead of exhibiting magnetic Bragg peaks on a zone boundary of its bcc crystal structure, such Bragg peaks are found in neutron scattering experiments at positions that are related by cubic symmetry to the wavevector $(1 - \delta, 0, 0)$, with $\delta \approx 0.05$, as shown in Figure 1.

The magnetic Bragg reflections are a manifestation of a spin density wave (SDW) that is favoured as the ground electronic state because it causes an energy gap on two large, nearly parallel sheets of Fermi surface [2,3,4]. It took many years of careful research to find tiny second and third-order harmonics of the primary SDW Bragg reflections [5]. These satellites are so weak that, for all intents and purposes, one may consider the SDW to be sinusoidal.

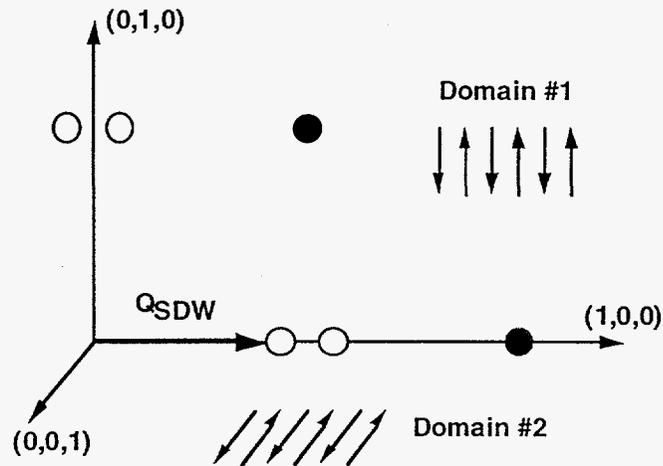


Figure 1: The chromium reciprocal lattice with nuclear Bragg peaks (filled circles) $(2,0,0)$ and $(1,1,0)$ and magnetic satellites (open circles) at $(1\pm\delta, 0, 0)$ and $(\pm\delta, 1, 0)$. The SDW wavevector of a single-Q state is shown, as are the antiferromagnetic spin orientations of the two plane-polarized TSDW domains corresponding to that SDW wavevector.

Immediately below the Neel temperature, the SDW appears to be perfectly plane-polarized with electronic spins directed perpendicular to the SDW wavevector, Q_{SDW} . In this so-called transverse spin density wave (TSDW) state, the spin polarization is preferentially directed along one of the cube edges of the crystal structure. In a crystal that is not specially prepared, all symmetry related variants of the SDW wavevector and its plane of polarization are present, so neutron scattering experiments see satellites at all positions related by symmetry to $(1-\delta, 0, 0)$.

It is possible by careful sample preparation to produce a sample with a single TSDW wavevector and a dominant spin-polarization state. To do this, one first cools a (almost perfect) single crystal of chromium through T_N in a large magnetic field ($H \sim 12$ Tesla for the experiments reported here) directed along one of the cube edges, which we will take as the $(1,0,0)$ direction. This has the effect of stabilizing the TSDW whose wavevector is parallel to the applied field. Once the crystal is securely in the TSDW phase below T_N , this field can be removed without changing the single-Q state. The degree to which a single-Q state is achieved can be judged by measuring the relative intensities of the $(1-\delta, 0, 0)$ and $(0, 1-\delta, 0)$ satellites, and is usually 99% or more.

Once a single-Q state has been stabilized, a magnetic field of a few Tesla (we used 6 Tesla) applied along a cube edge perpendicular to Q_{SDW} (taken to be the direction $(0,0,1)$ in Figure 1) stabilizes the magnetic domain with polarization in the plane of Figure 1 (i.e. a domain with spins directed alternately along $\pm(0,1,0)$ directions). Unlike the field used to stabilise the single-Q state, however, removal of the polarizing field allows an immediate reappearance of spin domains polarized along $\pm(0,0,1)$. The field required to assure strong selection of a single polarization domain is sample-dependent, probably because the field has to compete with defects that pin spins [6].

A sample prepared in the manner described above has three types of magnetic satellite reflections, as shown in Figure 2. The "visible" satellites are those which correspond to the selected domain with Q_{SDW} along $(1,0,0)$ and spins alternately along $\pm(0,1,0)$. "Silent" satellites are those which are absent because the sample has been prepared in a single-Q state with Q_{SDW} along $(1,0,0)$. In this situation, satellites corresponding to domains with Q_{SDW} along $(0,1,0)$ or $(0,0,1)$ cannot be observed. Finally, there are satellites which are "suppressed" by the strong field which is applied along $(0,0,1)$ during the experiment. Because neutron scattering can only observe magnetic scattering from components of magnetization that are perpendicular to the wavevector transfer used in an experiment, the fact that the applied field favours the TSDW domain with spins along $\pm(0,1,0)$ means that satellites at $(\pm\delta,1,0)$ are "suppressed" because the ordered moments are almost parallel to the wavevector transfer.

We have chosen to give the weaker satellites different names (i.e. "silent" and "suppressed"), both to distinguish the physical origin of their low intensities and also because the magnetic field applied along $(0,0,1)$ during the experiments does not fully extinguish the "suppressed" satellites. Nevertheless, as Figure 3 demonstrates, there is a considerable difference between the populations of the $(0,1,0)$ and $(0,0,1)$ polarized domains at all temperatures in the TSDW phase in our experiments.

3. Neutron Scattering with Polarization Analysis

Most of our knowledge about the magnetic structure of chromium has been derived from neutron scattering experiments. The fact that neutrons have a magnetic interaction with unpaired electron spins whose magnitude is similar to the nuclear interaction between neutrons and matter is one reason for this. Another is that chromium has a collectively organized magnetic ground state, a spin density wave, which gives rise to a neutron scattering pattern that is well-localized in reciprocal space, and thus easily measurable with a conventional neutron diffractometer.

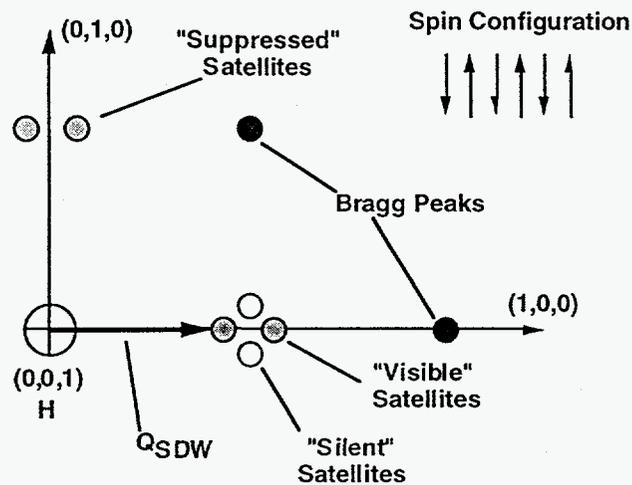


Figure 2: This figure shows the location of the "visible", "silent", and "suppressed" magnetic satellites described in the text.

To sort out the magnetic structure it is useful to add neutron polarization analysis [7,8] to neutron scattering experiments, because this technique is able to distinguish between scattering from various components of sample magnetization. The rules which govern neutron polarization analysis are:

1. as a result of the dipolar nature of the interaction between neutrons and sample magnetization, the scattering is sensitive to the Fourier component, $M_{\perp}(q)$, of magnetization that is perpendicular to the neutron wavevector transfer used in the experiment (we have already seen above how this fact causes certain satellites to be "suppressed").
2. when magnetic neutron scattering does not alter the spin state of the neutron — so-called non-spin-flip scattering (NSF) — only the component of $M_{\perp}(q)$ along the spin quantisation direction of the neutron is measured. In an experiment, the spin quantisation direction is defined by a magnetic field (which may be as small as 10 Oersted) applied to the sample.
3. if the neutron spin is inverted with respect to the neutron spin quantisation direction during the scattering process — a process known as spin-flip scattering (SF) — components of $M_{\perp}(q)$ that are *perpendicular* to the quantisation direction are responsible for the observed neutron scattering.

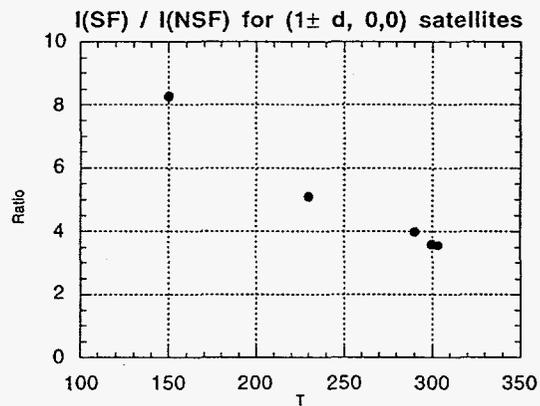


Figure 3: Intensity ratio of spin-flip to non-spin-flip scattering observed for the $(1\pm\delta, 0, 0)$ satellites as a function of temperature.

As an example of the application of this method, consider the data shown in Figure 3 which was obtained using the IN20 spectrometer at the Institut Laue-Langevin in Grenoble, France. Because a strong magnetic field is applied along the $(0, 0, 1)$ direction of the sample (cf. Figure 2), the ratio of SF to NSF scattering at $(1\pm\delta, 0, 0)$ satellites essentially tells us the ratio of the populations of static spin domains whose spins are along the $\pm(0, 1, 0)$ and $\pm(0, 0, 1)$ directions respectively. As can be seen from Figure 3, the applied magnetic field of 6 Tesla does not completely suppress the domain with $\pm(0, 0, 1)$ spin polarization but, nevertheless, this domain is at least four times less populated than the $\pm(0, 1, 0)$ domain at all temperatures where measurements have been made in the TSDW phase.

4. Spin Waves?

If chromium were an antiferromagnetic insulator, one would expect to observe spin waves with linear dispersion close to the antiferromagnetic Bragg peaks. When about 5% manganese is added to chromium, the SDW wavevector can be made commensurate and steep spin waves are apparently seen. In pure chromium the story is very different (perhaps casting some doubt on the interpretation of the Cr5%Mn data!)

In Figure 4 we display the result of a constant energy scan with energy transfer of 4 meV taken along the $(QH, 0, 0)$ direction of chromium at a temperature of 230K. The geometry used was that summarized in Figure 2, with a 6 Tesla field directed along $(0, 0, 1)$.

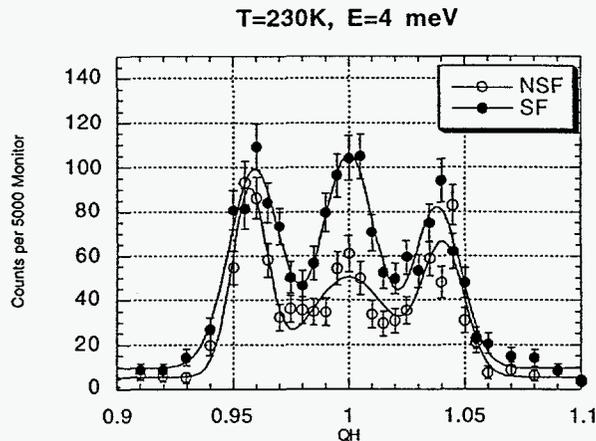


Figure 4: Constant energy scan at $E = 4$ meV, as described in the text. The lines are fits to three Gaussian peaks

Several things are clear from Figure 4:

1. Both the SF and the NSF scattering have a three-peaked form with a commensurate peak at $QH = 1$ and incommensurate peaks at $QH \approx 0.96$ and $QH \approx 1.04$. The latter peaks, it turns out, are at wavevectors close to (but not at) the elastic satellite positions.
2. The positions and peak intensities of the NSF and SF incommensurate peaks are similar but the NSF peaks appear to be somewhat narrower. The instrumental resolution is about 0.01 reciprocal lattice units, so both types of peaks have intrinsic width.
3. The commensurate peak (i.e. the one at $QH = 1$) is much stronger in the SF channel than it is in the NSF channel.

In an unpolarized neutron experiment, one would simply record the sum of the SF and NSF intensities in Figure 4 and deduce that the incommensurate peaks were very steep spin wave modes emanating from the SDW satellites. Figure 4 shows that this is not the case, because spin waves would be expected *only* in the NSF channel for a sample prepared as in Figure 2. What we have observed are roughly equally intense *transverse* and *longitudinal* fluctuations, i.e. magnetic fluctuations close to the satellite wavevectors that are both perpendicular (in the NSF channel) and parallel (in the SF channel) to the ordered TSDW moments that are directed along $\pm(0,1,0)$. Moreover, the intensities of these incommensurate inelastic peaks are roughly equal, even though the elastic scattering at the satellite wavevector displays a difference of a factor of about 5 between SF and NSF intensities at $T = 230\text{K}$ (cf. Figure 3).

A further observation that belies the spin-wave explanation of the inelastic neutron scattering is that both the NSF and SF incommensurate peaks move closer to $QH = 1$

with increasing energy transfer. If these peaks represented very steep spin waves, one would expect them to broaden with increasing energy transfer, but remain centred at the elastic satellite positions.

5. The Commensurate Excitation

The 4-meV inelastic peak at the commensurate ($QH = 1$) position in Figure 5 was first observed by Fincher et al [9] using unpolarized neutrons. These authors proposed that the peak might be due to counter-oscillating blocks of spins. They postulated that the SDW could be viewed as blocks of relatively strongly correlated spins joined, at the nodes of the SDW, by relatively weak interactions, as shown in Figure 5. In this case, it was suggested, each block of spins would be free to oscillate easily about the direction of the SDW wavevector, giving rise, according to the rules of neutron polarization analysis enumerated above, to a commensurate peak in the NSF channel.

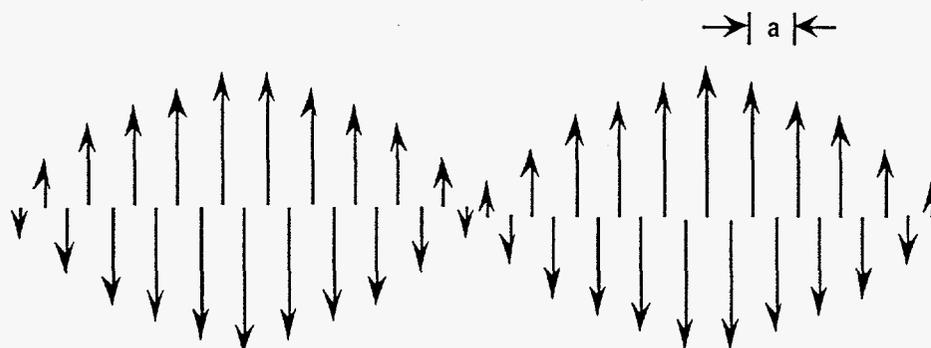


Figure 5: Schematic diagram of the chromium TSDW showing the spatial variation of spins at the chromium atomic sites.

Clearly, according to Figure 4, the commensurate peak is more strongly visible in the SF channel than in the NSF. Thus, the principal source of scattering is unlikely to be the twisting block mode proposed by Fincher et al.

Following the first observation of the commensurate inelastic scattering, Burke et al [10] examined this scattering in more detail, again using unpolarized neutrons, and observed more structure than is evident in Figure 4. Data similar to that measured by Burke et al, but taken with full neutron polarization analysis, are shown in Figure 6. These data and similar results at higher temperatures show that:

1. At 6 meV transfer, the SF commensurate excitation has split into two peaks, peaked at $QH = 0.8$ and $QH = 1.02$.

2. Although both the NSF and SF commensurate scattering in the 2 meV data shown in Figure 6 can be fit reasonably well with a single Gaussian peak, this becomes impossible at higher temperatures because there is conflict between the required (large) width of the commensurate peak and the sharp drop-off of the scattering at the outer edges of the incommensurate peaks. This observation casts doubt on the assertion that the scattering centred at $(1,0,0)$ at 2 meV is really a single commensurate peak.

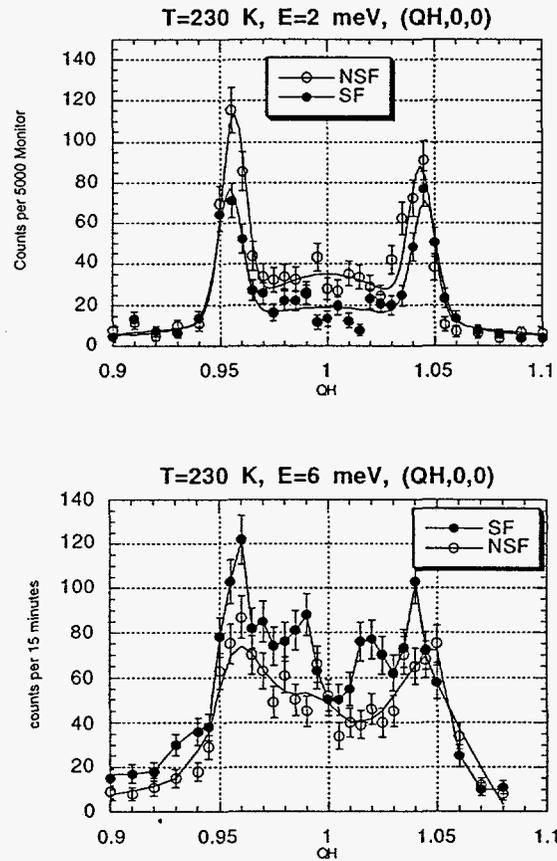


Figure 6: $(QH,0,0)$ scans at 2 meV (upper panel) and 6 meV (lower panel) energy transfer. Lines through the points are guides to the eye for the 6 meV data and Gaussian fits to 3 peaks at 2 meV.

Burke et al reported that their observations were consistent with the dispersion curves shown in Figure 7 although, without polarized neutrons, they were unable to deduce the spin polarization of the modes they saw. Because the dashed excitations in Figure 7 had the same slope as $(1,0,0)$ longitudinal acoustic (LA) phonon branches, Burke et al postulated that these branches corresponded to magneto-elastic scattering, that is to LA

phonons seen because each of the chromium atoms is supposed to rigidly carry a magnetic moment with which the neutron can interact, as shown in Figure 5. It is clear from the rules for neutron polarization analysis discussed above that one would expect magneto-elastic scattering of this type to appear in the SF channel, because the scattering is observed via the ordered SDW moments. Evidently, the peaks in the SF channel of the lower panel of Figure 6 are consistent with this requirement.

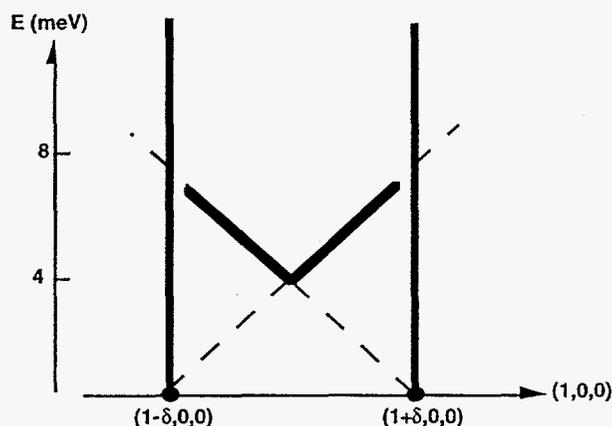


Figure 7: Dispersion relation postulated by Burke et al for low-energy excitations in chromium. Our experiments show that the steep modes emanating from the satellites involve both longitudinal and transverse magnetic fluctuations (i.e. fluctuation parallel and perpendicular to the TSDW ordered moments). The branches shown partly dashed are those whose slope is close to that of $(1,0,0)$ LA phonons. These branches are clearly visible only for the part of the branch that is depicted by the solid line.

However, before we unambiguously assign the dashed branches in Figure 7 to magneto-elastic scattering, it is worth noting, as did Burke et al, that such a mechanism totally fails to explain the rapid growth of intensity at the 4 meV mode crossing as temperature is increased towards the Neel point. As Greer et al [11] showed, this intensity increases essentially exponentially by a factor of about 10 between 230K and the Neel point, whereas the detailed balance factor can only account for an increase of less than 40% over this temperature range.

A further problem that we have discovered in our experiments is that it appears to be quite impossible to observe transverse acoustic phonons near the SDW satellites in spite of the fact that modes with reduced wavevector in the $(0,1,0)$ direction and atomic motions along $(1,0,0)$ would usually be easier to observe than longitudinal acoustic phonons propagating along $(1,0,0)$.

6. Critical Scattering

These conundrums were apparently resolved by Sternlieb et al [12] whose results appeared in Physical Review Letters just as we were completing our experiment using IN20. Using unpolarized neutrons, Sternlieb et al observed *inelastic* scattering at the

positions of "silent" satellites that increased dramatically in intensity as the Neel point was approached, in spite of the fact that there was no corresponding *elastic* scattering at these positions. Given the fact that we have observed inelastic scattering at wavevectors of "suppressed" satellites that has essentially equal intensity for longitudinal and transverse fluctuations (cf. Figure 4), this observation should perhaps not be a surprise.

Sternlieb et al explained their observed inelastic scattering as critical scattering associated with the Neel transition and asserted that, as a result of finite spectrometer resolution, this scattering explained fully the commensurate inelastic scattering in Figure 4. Their idea is based on the observation that there are "silent" satellite positions at $(1,0,\pm\delta)$ which, at any energy transfer, are included within the resolution of the spectrometer, which is usually poor in the direction perpendicular to the scattering plane.

Although the Sternlieb et al conjecture has the advantage of providing a natural explanation for the observed increase in intensity with temperature of the 4 meV commensurate mode, it is not without problems of its own.

1. Perhaps the most striking deficiency of their model is that it cannot explain the fact that the commensurate inelastic intensity breaks into two incommensurate modes at 6 meV as shown in the lower panel of Figure 6. The resolution effect postulated by Sternlieb et al *always* gives a commensurate peak at any energy transfer.
2. Another difficulty is that constant-Q scans at $(1,0,0)$ show a peak close to 4 meV, whereas there is no such peak in constant-Q scans at the satellite wavevectors. The resolution model requires there to be a peak at the same energy in each of these scans if it is to explain the data.

To further examine the explanation given by Sternlieb et al, we carried out constant-Q scans at $(1,0,0)$ and at $(1,0,\pm\delta)$, tilting the sample goniometer by a suitable amount to reach the second position. To reduce contamination from vertical spectrometer resolution in these scans, we also used flat monochromator and analyzer crystals (the majority of our data were taken with focusing Heusler monochromator and analyzer to increase the signal strength). Our data clearly show that, with full focusing of monochromator and analyzer, no more than one third of the commensurate 4 meV scattering in either the SF or the NSF channel at 230K can be explained by vertical spectrometer resolution.

A detailed Monte Carlo simulation of the spectrometer resolution shows that, at 4 meV energy transfer and 230K, the inelastic scattering at the $(1,0,\pm\delta)$ would need to be 64% of the scattering at allowed $(1\pm\delta,0,0)$ satellites to explain the NSF commensurate scattering and 90% of the corresponding allowed scattering to explain the SF commensurate scattering. The measurements of Sternlieb et al would lead one to

expect the inelastic scattering at "silent" satellites to be at most 15-20% of the scattering at the allowed satellite.

The result of these rather complex arguments is the following:

1. There is certainly a contribution centred at $QH = 1$ in both the SF and NSF channels in Figures 4 and 6. This contribution, which (probably) has the same Q -width and intensity in both SF and NSF channels, arises from inelastic scattering at the out-of-plane "silent" satellites being included in the spectrometer resolution when the scans in Figure 4 and 6 are made.
2. This critical scattering at the "silent" satellites explains the rapid temperature dependence of the commensurate inelastic scattering as the Neel point is approached.
3. In addition to the critical scattering there are excitation branches like the dotted ones in Figure 7, *at least* in the SF channel (corresponding to magnetic fluctuations parallel to the ordered moment).
4. There *may be* additional branches like the dotted ones in Figure 7 in the NSF channel (corresponding to magnetic fluctuations along $(0,0,1)$), but to determine this with certainty will require a reliable estimate of the "silent" satellite critical scattering to be subtracted from the measured NSF scattering.

None of these conclusions is really at odds with those of Sternlieb et al. The experiments they reported involved scans at 0.5 meV energy transfer and, as Figure 7 makes clear, there is likely to be very little contribution at this energy from the dotted mode in the Figure. It is likely true that the commensurate inelastic scattering at that energy transfer could be explained by a resolution effect in their data. Their mistake was in extrapolating this conclusion to *all* energy transfers.

Figure 8 shows that the NSF and SF scattering at $(1,0,0)$ and $(0,1,0)$ are generally very similar at all energies below 8 meV at a temperature of 290K. The exception is the SF scattering at $(1,0,0)$ which clearly shows additional intensity between 2 meV and 4 meV. If all of the commensurate scattering were a result of critical scattering at

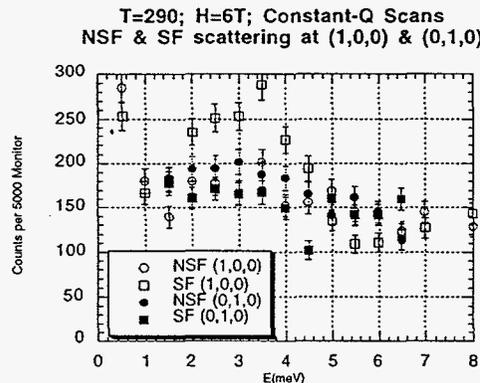


Figure 8: NSF and SF constant-Q scans at $(1,0,0)$ and $(0,1,0)$ at 290K

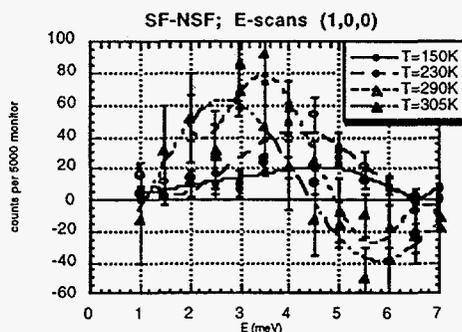


Figure 9: The difference between SF and NSF constant-Q scans at (1,0,0). Lines are guides to the eye.

“silent” satellites, one would expect all of the curves in Figure 8 to be the same. That they are not is a manifestation of the mode crossing at 4 meV shown in Figure 7.

The difference between the SF and NSF inelastic neutron scattering at (1,0,0) is plotted as a function temperature in Figure 9. Although the data are somewhat noisy, it does appear as if the crossing energy of the dashed lines in Figure 7 (i.e. the position of the peak in Figure 9) has a tendency to soften by as much as 40% as temperature is raised from 150K towards the Neel point. Over the same temperature range, the value of δ changes from $\delta \approx 0.047$ at 150 K to $\delta \approx 0.038$ at 300K, so one might expect the crossing energy to decrease by about $(0.047 - 0.038)/0.047 \approx 20\%$ even if the slope of the dotted branches in Figure 7 stayed constant with temperature. This seems to be a little less than indicated by Figure 9 but, given the noisiness of the data, is certainly not possible to conclude that it is inconsistent with what one sees in the Figure.

7. What does it all mean?

It is generally accepted that the SDW state of chromium is energetically favourable because the SDW wavevector pairs electron states in an octahedral pocket around the Γ point in the Brillouin zone with hole states in an octahedral pocket of slightly different size around the H point. This pairing mechanism leads to an energy gap at the Fermi surface which obeys a similar equation to that for the superconducting gap in BCS theory. Optical techniques allow this gap to be estimated at 150 meV.

Using this so-called two-band model, various authors have attempted to calculate the spectral form for magnetic fluctuations. The first to do so were Fedders and Martin [3] who replaced the actual Fermi surface with equal electron and hole spheres and predicted spin waves with linear dispersion emanating from the SDW satellites with a slope close to the Fermi velocity.

Later, Sato and Maki [13], using a model with different sized electron and hole Fermi surfaces again found steep spin waves but predicted that their velocity should go to zero as the Neel temperature was approached from below as $(T_N - T)^{1/2}$. These authors also examined the longitudinal spin susceptibility and calculated a spectral form for this function which they found to be very similar to that obtained for transverse (spin-wave) fluctuations, although the intensities of the longitudinal and transverse spectral functions were quite different.

Sokoloff [14] applied the random phase approximation to a Hubbard Hamiltonian and found the transverse spin fluctuations to be well defined spin waves emanating from the SDW satellites up to twice the energy of the gap introduced by the SDW, at which point he found a Stoner continuum. In Sokoloff's calculation there may be a well-defined pole in the longitudinal susceptibility but this mode is of finite frequency at the SDW satellite position.

Finally Zhu and Walker [15] wrote down a phenomenological free energy of the Landau type and again found transversely polarized spin waves, this time with an anisotropic dispersion. Their calculations also led to the conclusion that phase and amplitude excitations of the SDW are diffusive rather than propagating in nature.

Clearly, each and every one of these calculations gives predictions for the magnetic fluctuations in chromium which are not even qualitatively similar to the experimental data. They all predict well-defined classical spin waves while our observations and those of investigators before us are not consistent with a model in which collective modes, however steep, rise from the SDW satellites. With the (partial) exception of the calculation of Sato and Maki, none of the theoretical models predicts longitudinal fluctuations that are similar both in amplitude and spectral form to the transverse, spin-wave-like fluctuations. Finally, none of the models predicts additional longitudinally polarized modes with relatively low group velocity.

In our view, a possible interpretation of the very steep excitation branch emanating from the SDW satellites is that it corresponds to a triplet pairing of an electron and a hole excited close to the electron and hole Fermi surfaces around Γ and H. Within this model, it is not unreasonable that the excitations should be essentially spin-isotropic, independent of the magnetic field applied to the sample, because the Zeeman energy is simply not sufficient to influence the spin polarization of the excitation.

One model that might be worth considering for the low velocity modes in Figure 7 is that of the excitations of a soliton lattice of spins such as is induced in CuGeO_3 by a magnetic field (see the lectures by Broholm in this proceedings). The excitations described by Broholm certainly bear a qualitative resemblance to the LA-phonon-like modes we have seen and the SDW in that material is not dramatically different from that found in chromium. Alternatively, perhaps more detailed measurements will show

that the commensurate excitation is more localised in Q-space than Figure 7 might lead one to believe. In that case, perhaps intraband transitions might be able to explain it.

Clearly there is a number of further experimental measurements that might help to resolve some of the existing mysteries. Firstly, detailed measurement of the inelastic scattering at "silent" satellites and its dependence on neutron polarization is needed in order to be able to subtract this scattering from that at the commensurate position close to the "allowed" satellites. Such measurements will also check whether the scattering at the "silent" satellites is also isotropic in spin space as we observe at the "allowed" and "suppressed" satellites. Secondly, a more detailed study is needed of the dashed modes in Figure 7. Perhaps, if these modes are measured in the directions away from the commensurate point in Figure 7, one might be able to say with more precision whether the slope of the modes is identical to the that of LA phonons, or simply close to that value.

8. Conclusion

Forty years after the first neutron scattering measurements were made on chromium metal, we still do not understand the low-energy spin fluctuation in this body-centred cubic element!

References

- [1] For a comprehensive review see: E. Fawcett, (1988) *Rev. Mod. Phys.*, **60**, 209
- [2] W. M. Lomer, (1962) *Proc. Phys. Soc. London* **80**, 489
- [3] P. A. Fedders and P. C. Martin, (1966) *Phys. Rev.* **143**, 24
- [4] for a comprehensive list of references to microscopic models see K. Machida and M. Fulita, (1984) *Phys. Rev.* **B30**, 5284
- [5] R. Pynn, W. Press, S. M. Shapiro and S. A. Werner, (1976) *Phys. Rev.* **B13**, 295
- [6] S. A. Werner, A. Arrott, and M. Atoji, *J. Appl. Phys.* **40**, 1447
- [7] R.M. Moon, T. Riste, and W. C. Koehler, (1969) *Phys. Rev.* **181**, 920
- [8] R. Pynn, J-P. Boucher and L-P Regnault, (1989) *Physica* **B160**, 204
- [9] R. Fincher, Jr., G. Shirane, and S. A. Werner, (1981) *Phys. Rev.* **B24**, 1312
- [10] S. K. Burke, W. G. Stirling, K. R. A Ziebeck, and J. C. Booth, (1983) *Phys. Rev. Lett.* **51**, 494
- [11] B. H. Grier, G. Shirane, and S. A. Werner, (1985) *Phys. Rev.* **B31**, 2882
- [12] B. J. Sternlieb, J. P. Hill, T. Inami, and G. Shirane, (1995) *Phys. Rev. Lett.* **75**, 541
- [13] H. Sato and K. Maki, (1974) *Int. J. Mag.* **6**, 1983
- [14] J. B. Sokoloff, (1969) *Phys. Rev.* **185**, 770; *ibid* **185**, 783; *ibid* **187**, 584
- [15] X. Zhu and M. B. Walker, (1986) *Phys. Rev.* **B34**, 8064